

Narrowband ultraviolet B induces peripheral regulatory T cells to exert antigen-specific immune suppression

Chun-Hao Lu¹, Ching-Hui Tsai¹, Iquo O. Phillip¹, Pei-Chuan Chiang¹, Shao-Han Chang¹, Huan-Yuan Chen¹, Hao-Jui Weng², Pi-Hui Liang³, Shih-Yu Chen¹, Fu-Tong Liu¹, Tsen-Fang Tsai⁴, and Yungling Lee¹

¹Institute of Biomedical Sciences Academia Sinica

²Taipei Medical University

³National Taiwan University School of Pharmacy

⁴National Taiwan University Hospital Department of Dermatology

February 07, 2025

Abstract

Background: Commonly used to treat inflammatory skin diseases, narrowband ultraviolet B (UVB) has been shown to induce antigen-specific immune suppression when combined with alloantigen immunization, but the underlying mechanism remains elusive. **Methods:** We used cytometry by time-of-flight (CyTOF) to analyze the peripheral blood mononuclear cells (PBMCs) from 19 psoriasis patients enrolled in UVB trial. Mouse models of ovalbumin (OVA)-induced skin inflammation and allogeneic skin transplantation were used to investigate the effects of UVB on antigen-specific regulatory T cell (Treg) induction. We applied bulk RNA sequencing (RNA-seq) and single-cell RNA sequencing (scRNA-seq) methods to the analysis of mouse skin Tregs and PBMCs, respectively. **Results:** CyTOF analysis revealed patients' therapeutic response to be determined by a cluster of CD4⁺ T cells expressing T cell receptor (TCR)-activated and Treg-associated molecules. In clinical trial and mouse models of skin inflammation and allogeneic skin transplantation, UVB led to immunosuppressive phenotypes through antigen-specific Treg induction. RNA-seq from mouse skin Tregs showed that UVB enhanced gene expression associated with cell stability, cellular location, and cell proliferation. When compiling with human peripheral Tregs analyzed by scRNA-seq, we found similar gene expression patterns involved in Treg differentiation, maintenance, and function. Furthermore, scRNA-seq analysis also demonstrated that UVB inhibited negative regulators of Treg development, thereby promoting CD4⁺ T differentiation into Tregs, clonal expansion of which was also noted. **Conclusions:** Our findings suggest UVB can induce antigen-specific Tregs in a clinical setting, highlighting its potential for broader immunosuppressive applications.

1 INTRODUCTION

A commonly used therapy in dermatology, narrowband ultraviolet B (UVB) exerts immunosuppressive effects on the skin to attenuate central nervous system autoimmunity¹ and prevent atherosclerosis² by regulating systemic inflammatory responses. UVB-induced immunosuppression can be hapten-specific, based on a mouse model of hapten-induced contact hypersensitivity (CHS), where UVB suppressed skin phenotypes but skin sensitized to unrelated haptens remained unaffected.³ Results of a separate study where an injection of splenocytes from UVB-tolerized mice into naive mice also indicated skin phenotype suppression.⁴ Other studies have shown that UVB irradiation with alloantigen immunization can protect allografts from rejection.^{5,6} Even though UVB can induce peripheral tolerance to a specific antigen, the mechanism remains unclear.

Previous work has implicated the expansion of regulatory T cells (Tregs) by UVB.^{1,2,7,8} Various immune

responses, including autoimmunity, transplant rejection, antitumor immunity, and allergy⁹⁻¹¹, are suppressed by Tregs, of which there are two types: τηψμυσ-δερμειδ Τρεγς (τΤρεγς) ανδ περιπεραλ Τρεγς (πΤρεγς).¹² Τρεγ δεελοπμεντ ιν τη τηψμυσ ις ασσοσιατεδ ωιτη ηιγη-αφφινιτψ ιντεραστιον βετωεεν Τ^αΡ ανδ μαθορ ηιστοσομπατιβιλιτψ ζομπλεξ (ΜΗ^α)-πεπτιδε, ωηιλε πΤρεγ διφφερεντιατιον ιν τη περιπερψ ζαν βε ινδυσεδ υνδερ συβ-ιμμυνογενις ζονδιτιονς.^{13,14} Περιπεραλ Τρεγς αρε κνωων το πλαψ αν ινδισπενσαβλε ρολε ιν τη ζοντρολ οφ ιμμυνιτψ ατ ινφλαμματορψ τισσυε σιτες.^{15,16} Σομε στυδιες ηαε συγγεσσεδ τη ζονερσιον οφ μεμορψ ορ εφφεστορ Τ ζελλς το Τρεγς ιν ιτρο ανδ ιν περιπεραλ τισσυες. Κιμ ετ αλ. σηοωεδ τηατ αντιγεν-σπεσιφικς μεμορψ Τη2 ζελλς αρε ινδυσεδ το διφφερεντιατε ιντο Φοξπ3⁺ Τρεγς βψ ΤΓΦ-β, αλλ-τρανς ρετινοικς ασιδ, ανδ ραπαμψιν.¹⁷ Αμαρνατη ετ αλ. φουνδ τηατ ηυμαν Τη1 ζελλς αρε ζονερτεδ το Φοξπ3⁺ Τρεγς υνδερ προγραμμεδ δεατη λιγανδ-1 (ΠΔ-Α1) στιμυλατιον.¹⁸ Τηυς, πΤρεγς μαψ ζοντρολ λοζαλ ινφλαμματορψ ρεσπονσες, συζη ας ιν τηε σκιν, ανδ σηοω ζλινικαλ σιγνιφικανζε φορ αυτοιμμυνε δισηασες.

In the present study, we aimed to investigate the mechanism underlying the induction of antigen-specific Tregs by UVB, which confers peripheral tolerance to an antigen. We report the effects of UVB on human peripheral CD4⁺ T cells in a prospective UVB phototherapy trial using cytometry by time-of-flight (CyTOF). Mouse models of OVA-induced skin inflammation and allogeneic skin transplantation were used to validate antigen-specific Treg induction under UVB treatment. We performed adoptive transfer experiments to investigate the role of UVB-induced antigen-specific Tregs in disease modulation. Using single-cell RNA (scRNA) sequencing analysis, we sought to illustrate the detailed pathway of Treg differentiation from CD4⁺ T cells and understand how UVB induces antigen-specific Tregs in human peripheral tissues.

2 METHODS

Methods are described in Supplementary Methods.

3 RESULTS

3.1 A distinct cluster of CD4⁺ T cells dictates therapeutic response to psoriasis patients to treatment with UVB

Peripheral blood mononuclear cells (PBMCs) were isolated from 38 blood samples taken from 19 mild to severe psoriasis patients (Table S1) before and after phototherapy at the Department of Dermatology, National Taiwan University Hospital (NCT05636839) and analyzed using cytometry by time of flight (CyTOF). A total of 42 markers targeting surface molecules and transcription factors were measured. FlowSOM analysis identified distinct immune cell clusters within the PBMC population (Figure S1). We identified a cluster (cluster 11) of CD4⁺ T cells characterized by high expression of CD25, FOXP3, and low expression of CD127 (Figure 1A), which exhibited elevated levels of TIGIT, CTLA4, TIM3, CD39, and Helios, markers associated with regulatory T cell (Treg) activation (Figure 1B). Receiver operating characteristic (ROC) curves were applied to assess the discriminative ability for UVB response. A total of 7 responders out of the 19 recruited patients achieved an over 50% reduction in Psoriasis Area Severity Index (PASI) score. The area under the curve (AUC) for cluster 11 at baseline showed a significant prediction for therapeutic response in psoriasis (adjusted-AUC, 0.85; 95% confidence interval (CI), 0.65 to 1.00) (Figure 1C). We also found that UVB significantly increased the size of cluster 11, but not the other clusters (Figure 1D and Figure S2). This specific cluster was recapitulated using conventional manual gating on HLADR and TIGIT pre- and post-UVB treatment (P = 0.03, Figure 1E, upper) or HLADR and TIM3 (P = 0.04, Figure 1E lower), indicating the TCR activation phenotype of Tregs after UVB treatment. Our results suggest that UVB induces activated Tregs in an inflammatory context.

3.2 UVB induces OVA-specific Tregs in mouse model of OVA-induced skin inflammation

We hypothesized that UVB-induced activated Tregs are antigen-specific. To investigate the impact of UVB

on the induction of antigen-specific Tregs, we induced skin inflammation in mice using ovalbumin (OVA) as a model antigen; the experimental protocol is shown in Figure 2A. OVA stimulation caused significant skin inflammation, characterized by redness, increased transepidermal water loss (TEWL), epidermal thickening, and inflammatory responses, and all were alleviated by UVB treatment (Figure 2B-D). To assess immune responses, cells isolated from the skin were restimulated with PMA and ionomycin, and intracellular cytokine staining with flow cytometric analysis was performed. Increased frequencies of IL-4-, IL-5-, and IL-22-producing CD4⁺T cells (gated as shown in Figure S3A) were noted in OVA-stimulated mice, and UVB treatment significantly reduced these inflammatory T cells (Figure 2E). These findings demonstrate that UVB inhibits inflammation induced by a model antigen.

We further analyzed skin-draining lymph node (dLN) cells (Figure S3B). UVB increased the frequency of CD25⁺Foxp3⁺ Tregs and upregulated the expression of TCR-activation markers, including CD25, ICOS, CTLA-4, TIGIT, Tim3, CD39, and Helios (Figure 2F). Similar findings were also detected in the skin (Fig S3C). These findings suggested enhanced antigen specificity. To test this, we used OVA₃₂₃₋₃₃₉tetramers to identify OVA-specific Tregs (gated as shown in Figure S3D). We found that OVA-specific Tregs in UVB-treated mice were significantly increased (Figure 2G). To further investigate the role of Tregs in UVB-mediated immune suppression, we depleted Tregs in Foxp3^{DTR-GFP} mice using diphtheria toxin (Figure S4A). Treg depletion under UVB treatment exacerbated skin inflammation and increased IL-4-producing CD4⁺ T cells (Figure S4B-D). In summary, UVB-induced immunosuppression is mediated by an increase in antigen-specific Tregs.

3.3 UVB induces alloantigen-specific immunosuppression in mouse model of allogeneic skin transplantation

We employed a mouse model of allogeneic skin transplantation to further investigate the antigen-specific immunosuppression induced by UVB. Full-thickness tail skin grafts from C57BL/6 donor mice were transplanted onto the right chest of BALB/c recipient mice. Starting on day 5, recipient mice were exposed to UVB every other day for a total of 5 courses (Figure 3A). Graft rejection was defined as less than 20% viable tissue remaining. We found that allogeneic skin grafts underwent complete rejection around 30 days post-transplantation, while UVB-treated grafts exhibited delayed rejection kinetics (Figure 3B). Histological analysis revealed reduced immune cell infiltration in UVB-treated grafts (Figure 3C). We further isolated cells from the graft tissues for flow cytometric analyses and found UVB significantly increased the frequency of CD25⁺Foxp3⁺ Tregs with enhanced activation markers (ICOS and LAG-3) (Figure 3D). To determine whether UVB-induced immunosuppression in the skin is antigen-specific, a second skin graft (either C57BL/6 or C3H) was transplanted onto the left chest of recipient mice (Figure 3E). In mice without UVB treatment during the first graft, both second grafts (C57BL/6 and C3H) were rejected. However, in mice with UVB treatment during the first graft, the second C3H graft was rejected normally, but the second C57BL/6 graft exhibited prolonged survival (Figure 3F). These results underscore the role of UVB in inducing antigen-specific immunosuppression via antigen-activated Treg induction.

3.4 A specific cluster of Tregs, identified in peripheral CD4⁺ T cells, is inversely associated with disease severity

We hypothesized that cluster 11, primarily composed of activated Tregs, plays a critical role in modulating skin inflammation and is associated with psoriasis severity. To test this hypothesis, we analyzed 38 blood samples and found a negative correlation between the percentage of cluster 11 cells and PASI score (Figure 4A). Furthermore, when patients were categorized into low (PSAI [?] 4.5), medium (4.5 < PASI < 9), and high (PASI [?] 9) PASI groups, those with high PASI scores exhibited the lowest percentage of cluster 11 compared to healthy controls (Figure 4B). These findings suggest that a higher proportion of the activated Tregs, represented by cluster 11, may contribute to reduced skin inflammation in psoriasis patients.

3.5 UVB-induced antigen-specific Tregs influence the clinical outcomes

To confirm the role of UVB-induced antigen-specific Tregs in disease modulation, we performed adoptive transfer experiments. Live GFP⁺ Tregs were sorted from the skin-draining LNs of Foxp3^{DTR-GFP} mice

under conditions of OVA-induced skin inflammation (Figure 4C and Figure S5A). Naive CD4⁺CD25⁻GFP⁻ T cells (naive T cells) were sorted from OT-II/Foxp3^{DTR-GFP} mice. A 1:1 mixture of Tregs and naive T cells was intravenously injected into recipient mice one day before sensitization with OVA/Alum followed by OVA patch challenges (Figure 4C). OVA-stimulated mice receiving naive T cells demonstrated significant skin inflammation and an influx of IL-5-producing CD4⁺ T cells into the skin. Neither Tregs from UVB-irradiated mice without OVA stimulation (UTregs) nor Tregs from OVA-stimulated mice without UVB treatment (OTregs) were able to prevent OVA-induced skin inflammation in recipient mice. However, Tregs from OVA-stimulated mice treated with UVB (O+UTregs) significantly mitigated these inflammatory responses (Figure 4D-F).

In mouse model of imiquimod (IMQ)-induced psoriasiform dermatitis, Tregs were intravenously administered to recipient mice one day before topical application of IMQ to the ears (Figure 4G). We found that neither UTregs, OTregs, nor O+UTregs could suppress the inflammation of skin infiltrated with IL-17- and IL-22-producing CD4⁺ T cells (Figure 4H,I). These findings demonstrate that UVB-induced antigen-specific Tregs are critical for clinical phenotypes of skin inflammatory diseases.

We further performed in vitro suppression assays to investigate the functional properties of these Treg populations. **Bone marrow-derived dendritic cells (BMDCs) were generated from C57BL/6 mice and stimulated with LPS and OVA. UTregs, OTregs, and O+UTregs were assessed for their ability to inhibit BMDC activation and T-cell proliferation.** (Figure S5B). **All three Treg populations exhibited comparable inhibitory effects on LPS-induced BMDC activation. However, O+UTregs demonstrated a stronger ability to suppress BMDC activation in the presence of OVA** (Figure S5C,D). **Similarly, O+UTregs showed a higher ability to suppress the proliferation of naive OT-II T cells stimulated by OVA-pulsed BMDCs** (Figure S5E).

3.6 UVB inhibits negative regulators and activates functional and developmental genes to promote Treg induction

To study the mechanisms underlying the effects of UVB on antigen-specific Treg induction, we collected Tregs from UVB-untreated/treated skin of mice with imiquimod-induced psoriasiform dermatitis. RNA sequencing (RNA-seq) of Tregs from two independent experiments of UVB-untreated and treated skin samples was performed to investigate differentially expressed genes (DEGs) related to UVB treatment. Compared to UVB-untreated Tregs, UVB-treated Tregs showed alterations in 880 upregulated DEGs and 243 downregulated DEGs, after false discovery rate (FDR <0.05) correction and $|\log_2\text{-fold change}| \geq 1$. Principle component analysis (PCA) unveiled an altered transcriptional profile in UVB-treated Tregs relative to UVB-untreated Tregs (Figure S6A). Gene ontology analysis of the significantly upregulated DEGs revealed biological functions of cellular homeostasis, cell proliferation, and cell motility (Figure 5A). These findings suggest that UVB-treated Tregs show stable cell fate, high proliferative ability, and sustainable cellular location in the skin.

We performed single-cell RNA sequencing (scRNA-seq) on blood samples from two psoriasis patients whose disease was greatly mitigated by UVB treatment to investigate the underlying molecular mechanisms. Samples from the two patients yielded 4,832 CD4⁺ T cells, averaging 39,811 genes per cell, and comprised of 3,045 and 1,787 CD4⁺ T cells, which were well-distributed across the UMAP (Figure S6B). No distribution bias across cell clusters was evident in either the pre- (n = 2,502) or post-UVB (n = 2,330) treatment cells (Figure 5B). Subsequent analysis of CD4⁺ T cell phenotypic heterogeneity identified several clusters, which were annotated as naive T, T memory (Tmem), T effector (Teff), and Tregs based on known gene markers (Figure 5C). We identified different gene profiles between Tregs derived from UVB-untreated/treated skin of mice and before UVB/after UVB human blood samples, respectively (Figure 5D). Thirty-one genes were identified and were categorized into three gene sets. The first gene set, including *FOXO3*, *AHR*, and *SP1*, is involved in Treg differentiation, maintenance, and function. These genes were upregulated in both mouse skin and human blood Tregs upon UVB treatment, indicating Treg cellular functional improvement. The second gene set is classified as negative regulators. These genes were downregulated upon UVB treatment, supporting the examined Treg cell expansion. Notably, the changes in the expression of *IDH1* (p = 0.03),

VAV1 ($p = 0.02$), and *RAB35* ($p = 0.04$) were significant, a finding that merits further mechanistic investigation (Figure 5D,E). The last gene set, including *HAVCR2*, *NFKB1*, and *TIGIT*, is involved in TCR activation. Most of these genes were upregulated upon UVB treatment (Figure 5D). Overall, these genes indicate that UVB promotes Treg differentiation and expansion by cultivating Treg functional and developmental genes and inhibiting negative regulators.

3.7 Tregs in human peripheral blood are transitioned from naive CD4⁺ T cells

To further investigate the underlying mechanism of Treg induction from blood samples of patients under UVB treatment by scRNA-seq (Figure 5B,C), slingshot analysis was undertaken to infer cell lineages and pseudotimes and revealed a trajectory originating from naive T cells, transitioning into Tmem or Teff cells, and ultimately differentiating into Tregs (Figure 6A). A similar trajectory was also noted in human skin CD4⁺ T cells, as annotated in Figure S7A,B, although the skin contained few naive T cells (Figure 6B). This trajectory was corroborated by the chronologically colored pseudotime gradient map from Monocle3, with naive T cells represented by a dark violet hue, Tmem and Teff cells by purple to purplish-orange hues, and Tregs by orange to yellow colors (Figure 6C). Marker gene expression patterns along the trajectory confirmed the annotated cell functions (Figure 6D). Treg transcription factors (*FOXP3*, *IKZF2*, and *AHR*) and TCR activation markers (*IL2RA*, *TIGIT*, and *ICOS*) exhibited increased expression throughout the lineage. Notably, the steep upregulation of *FOXP3* and *IL2RA*, encoding Foxp3 and CD25, respectively, confirmed the Treg transition. Tmem and Teff markers (*CD44* and *CD69*) peaked at pseudotime Teff cells. Their subsequent decline indicated the transition to a Treg phenotype. Interestingly, the Treg negative regulator *CD226* followed a similar trend as Tmem and Teff markers, suggesting its potential involvement in Treg differentiation. Conversely, *SATB1* expression decreased gradually throughout the lineage, with the lowest expression in Tregs, indicating a reduction of its suppressive function. These findings collectively demonstrate that naive T cells differentiate into Tmem and Teff cells, which can further differentiate into Tregs.

3.8 UVB enhances Treg clonal expansion in human peripheral blood

To further validate Treg expansion induced by UVB, we integrated scRNA-seq and TCR VDJ sequencing data obtained from peripheral blood samples from the above two psoriasis patients, focusing on CD4⁺ T cells. We identified four distinct populations — naive T cells, T effector cells, T memory cells, and Tregs (Figure 6E, left) — of which a more condensed Treg population was observed after UVB treatment, suggesting clonal expansion (Figure 6E, right). To quantify this, we categorized clonotypes based on the number of cells expressing each TCR sequence: single ($0 < X \leq 1$), small ($1 < X \leq 5$), and medium ($5 < X \leq 20$). The proportion of small-to-medium clonal expansions increased within the Treg cluster post-UVB treatment (from 5.26% to 11.42%) (Figure 6F). Additionally, we calculated expansion indices using the Shannon entropy-based STARTRAC method. In both patients, a higher expansion index was noted in post-UVB Tregs compared to pre-UVB Tregs (Figure 6G). In conclusion, our TCR sequencing analysis demonstrates that UVB induces clonal expansion in human peripheral Tregs.

DISCUSSION

This study integrates human clinical data, transcriptomic analyses, and mouse models to investigate the effect of UVB on antigen-specific Treg induction. Our results demonstrate that UVB promotes the differentiation of antigen-activated CD4⁺ T cells into Tregs and enhances Treg clonal expansion, leading to antigen-specific immune suppression. By analyzing PBMCs from psoriasis patients by CyTOF, we identified a distinct CD4⁺ T cell cluster expressing Treg-associated molecules and TCR activation phenotypes (Foxp3, CD25, HLA-DR, TIGIT, and Tim3), which significantly increased after UVB treatment and predicted therapeutic response. This cell subset was further confirmed to be antigen-specific Tregs induced by UVB in mouse models of OVA-induced skin inflammation and allogeneic skin transplantation. Adoptive transfer experiments demonstrated the important role of UVB-induced antigen-specific Tregs in disease modulation. Finally, scRNA-seq and scTCR-seq analyses from patient PBMCs revealed that UVB treatment led to Treg differentiation from CD4⁺ T cells and Treg clonal expansion.

UVB irradiation can induce immune tolerance and effectively treat inflammatory skin diseases.¹⁹⁻²¹ The mechanisms underlying UVB-induced immunosuppression are multifactorial and complex. Immediate effects, including DNA damage, membrane lipid oxidation, and isomerization of chromophores (such as urocanic acid), induce cell growth arrest and apoptosis.^{22,23} Delayed effects include decreased inflammatory cytokine production, inhibition of antigen-presenting cell (APC) activity, and induction of Tregs.^{7,24} **In our results, we found UVB treatment increased the frequency of a specific cluster of Tregs (cluster 11) expressing significantly higher HLADR, TIGIT, and TIM3, the constitutional TCR activation markers, in psoriasis patients (Figure 1D,E). The induction of antigen-specific Tregs by UVB was further proved by using OVA tetramers in a mouse model of OVA-induced skin inflammation (Figure 2G), as well as by an animal model of allogeneic skin transplantation (Figure 3). These results show that UVB can significantly induce antigen-specific Tregs in the periphery to exert antigen-specific immune suppression in an inflammatory context.**

The therapeutic potential of Tregs has generated significant enthusiasm, in part due to the targeted suppression capabilities of antigen-specific Tregs, which avoid the global immunosuppression mediated by polyclonal Tregs. It is well known that TGF- β can increase Foxp3 expression in naive T cell subsets, including Th1, Th17, and Treg subsets.^{25,26} The TGF- β -dependent Foxp3 expression is not attenuated by proinflammatory cytokines.^{25,26} Akamatsu *et al.* reported that the inhibitory cytokine Δ K8/19 converts antigen-specific effector/memory T cells into Foxp3-expressing Tregs.²⁷ The converted Tregs suppress allergic immune responses in animal models.²⁷ Our adoptive transfer experiments found mice receiving OVA-induced OVA-specific Tregs did not develop skin inflammation under OVA stimulation conditions, indicating the suppressive effect of Foxp3-expressing Tregs on skin inflammation (Figure 4). By single-cell trajectory and pseudotime analyses on patient PBMCs, we found a trajectory originating from naive T cells, transitioning into Tmem or Treg cells, and ultimately differentiating into Tregs (Figure 6A). This was confirmed by analyzing CD4⁺ T cells in the skin (Figure 6B), as well as by the pseudotime analysis (Figure 6C,D).

UVB has numerous effects on local and systemic immunity. Our findings in mice indicated that UVB suppressed immune responses to topically applied model antigens by inducing antigen-specific Tregs. Several other studies have reported the systemic immunosuppression of UVB — Sasaki *et al.* found that UVB exposure prevented atherosclerosis in atherosclerotic mice⁸; Hayashi *et al.* suggested that UVB exposure suppressed angiotensin II-induced abdominal aortic aneurysm in mice by expanding Tregs²; and Breuer *et al.* indicated that UVB attenuated the systemic immune response in the central nervous system.¹ To better understand whether Tregs induced in the local site are similar to circulating Tregs, we undertook bulk RNA sequencing from skin-sorted Tregs in imiquimod-induced psoriasiform mice. With pathway analysis, we found DEGs associated with biological functions related to cell stability, cellular localization, and cell proliferation were upregulated in skin Tregs of UVB-treated mice (Figure 5A). When compiling the results with the RNA-seq profiles from patient PBMCs, we found similar expression patterns in genes involved in both positive and negative regulation of Treg differentiation, maintenance, and function, as well as in TCR activation signaling (Figure 5D,E).

Transcriptomic analysis of mouse skin and human blood Tregs under UVB treatment revealed three significantly down-regulated genes, including *VAV1*, *IDH1*, and *RAB35* (Figure 5E). The *VAV1* gene encodes the guanine

nucleotide exchange factor and is essential for transducing T cell receptor signals, suggesting its critical role in the development and activation of T cells.^{28,29} *VAV1*^{-/-} mice were resistant to MOG-induced experimental autoimmune encephalomyelitis (EAE) due to defective priming and expansion of CD4⁺ and CD8⁺ T cells.³⁰ The *IDH1* gene encodes isocitrate dehydroge-

nase 1, which catalyzes the NADP-dependent conversion of isocitrate to α -ketoglutarate. *Xu et al.* reported that knockdown of both *IDH1* and *IDH2* reduced Th17 cell differentiation and increased Foxp3 expression.³¹ *Aso et al.* suggested that itaconate inhibited IDH1/2, which altered the chromatin accessibility of essential transcription factors at *IL-17a* and *Foxp3 loci*, leading to decreased IL-17A and increased Foxp3 expression.³² The *RAB35* gene encodes Ras-related protein functioning in vesicle formation, motility, docking, and fusion.^{33,34} *Yang et al.* reported that Th2 cells deficient in Rab35 exhibited enhanced TCR-mediated effector function.³⁵ Previous studies suggested that the differentiation and function of Tregs are correlated with the strength of TCR signaling.³⁶⁻³⁸ Our study found UVB significantly inhibited these three negative regulators, which may affect TCR signaling during the antigen stimulation and result in Treg differentiation.

Single-cell TCR sequencing from patient PBMCs revealed that UVB enhanced clonal expansion in Tregs (Figure 6E-G). Compared to other T cell subsets (naive T, memory T, and effector T cells), Tregs exhibited a greater increase in clone size after UVB treatment, suggesting potential induction from other CD4⁺ T cells (Figure 6F). Analysis of individual samples demonstrated clonal expansion of Tregs in all cases (Figure 6G). The importance of clonal expansion of antigen-specific Tregs has been shown in patients with diabetes.³⁹ Specifically, individuals with long-standing anti-islet autoimmunity who do not progress to overt diabetes exhibit a higher frequency of insulin-specific Tregs compared to both healthy individuals and those with diabetes onset.³⁹

The relatively small sample size of psoriasis patients in UVB trial constrains our high-dimensional genomic data analyses. While clinical responses to UVB vary among individuals, CyTOF analysis from PBMCs revealed a statistically significant increase in activated Tregs post-UVB treatment (Figure 1D). While the role of Tregs in psoriasis remains debated⁴⁰⁻⁴², we observed a negative correlation between the proportion of activated Tregs and psoriasis severity in a significant dose-dependent manner (Figure 4A,B). The limited input cell numbers for scRNA and scTCR sequencing affected the depth of the transcriptomic analysis and the assessment of clonal expansion. Nevertheless, integrating genomic data from mouse and human samples sheds light on the differential gene expression patterns and offers a better understanding of the mechanism underlying the induction of antigen-specific Tregs by UVB.

In conclusion, our study provides evidence that the proportion of activated Tregs in peripheral blood may predict individual responses in UVB trial. Our scRNA/scTCR sequencing findings demonstrate that UVB exposure can induce Treg differentiation from other CD4⁺ T cell subsets and stimulate Treg clonal expansion, providing a novel mechanism underlying UVB-mediated antigen-specific immune suppression. The three significantly downregulated genes (*VAV1*, *IDH1*, and *Rab35*) represent potential therapeutic targets to induce antigen-specific Tregs in future translational studies.

STUDY APPROVAL

Whole blood samples were collected from psoriasis patients before and after UVB treatment and healthy volunteers who provided written informed consent (IRB protocol: 202301143RINB). Mouse experimental procedures were reviewed and approved by the Institutional Animal Care and Use Committee of Academia Sinica (Protocol number: 24-10-2305).

DATA AVAILABILITY

All data associated with this study are present in the paper or the supplementary materials. RNA sequencing data from human peripheral blood (GSE285339) and mouse skin Tregs (GSE285340) have been deposited in NCBI's Gene Expression Omnibus.

AUTHOR CONTRIBUTIONS

CHL and CHT conducted the clinical study, performed the experiments, analyzed the data, and wrote the manuscript. CHL designed and performed in vitro and in vivo mice experiments and analyzed the

data. IOP helped the in vitro experiments of the Treg suppression assay. PCC helped the in vivo animal experiments. TFT and HJW conducted the clinical trial and collected clinical samples. SYC provided advice about experiments of CyTOF and scRNA analysis. HYC and SHC helped with sample preparation for CyTOF. FTL and PHL provided advice about the interpretation of the data and revised the manuscript. YLL conceived and initiated the project, designed the study, raised the grant funding, and revised the manuscript. All authors edited, approved, and provided critical comments on the manuscript.

ACKNOWLEDGEMENTS

The authors thank the clinical assistants and dermatologists who supported data collection and all of the subjects who participated in this study. We also thank the NGS High Throughput Genomics Core, Flow Cytometry Core Facility (AS-CFII-111-212), Pathology Core, Experimental Animal Facilities, and the Inflammation Core Facility from Academia Sinica for the technical support.

FUNDING INFORMATION

This study was supported by the 2021-2022, 2024-2025 Postdoctoral Scholars from Academia Sinica (to CHT), grants UN112-0020 and UN111-0056 (to PHL and TFT) from the National Taiwan University Hospital, and grants IBMS-CRC112-P02 from Academia Sinica (to YLL).

CONFLICT OF INTEREST STATEMENT

TFT has conducted clinical trials or received honoraria for serving as a consultant for AbbVie, Anaptys-Bio, Bristol-Myers Squibb, Boehringer Ingelheim, Celgene, Eli Lilly, Galderma, GalaxoSmithKline-Stiefel, Janssen-Cilag, Leo-Pharma, Merck, Novartis, PharmaEssentia, Pfizer, Sanofi, Sun Pharma, and UCB. Other authors have declared that no conflict of interest exists.

REFERENCES

1. Breuer J, Schwab N, Schneider-Hohendorf T, et al. Ultraviolet B light attenuates the systemic immune response in central nervous system autoimmunity. *Ann Neurol.* 2014;75(5):739-758.
2. Hayashi T, Sasaki N, Yamashita T, et al. Ultraviolet B Exposure Inhibits Angiotensin II-Induced Abdominal Aortic Aneurysm Formation in Mice by Expanding CD4(+)Foxp3(+) Regulatory T Cells. *J Am Heart Assoc.* 2017;6(9).
3. Toews GB, Bergstresser PR, Streilein JW. Epidermal Langerhans cell density determines whether contact hypersensitivity or unresponsiveness follows skin painting with DNFB. *J Immunol.* 1980;124(1):445-453.
4. Elmetts CA, Bergstresser PR, Tigelaar RE, Wood PJ, Streilein JW. Analysis of the mechanism of unresponsiveness produced by haptens painted on skin exposed to low dose ultraviolet radiation. *J Exp Med.* 1983;158(3):781-794.
5. Ullrich SE, Magee M. Specific suppression of allograft rejection after treatment of recipient mice with ultraviolet radiation and allogeneic spleen cells. *Transplantation.* 1988;46(1):115-119.
6. Hori T, Kuribayashi K, Uemoto S, et al. Alloantigen-specific prolongation of allograft survival in recipient mice treated by alloantigen immunization following ultraviolet-B irradiation. *Transpl Immunol.* 2008;19(1):45-54.
7. Yamazaki S, Odanaka M, Nishioka A, et al. Ultraviolet B-Induced Maturation of CD11b-Type Langerin(-) Dendritic Cells Controls the Expansion of Foxp3(+) Regulatory T Cells in the Skin. *J Immunol.* 2018;200(1):119-129.
8. Sasaki N, Yamashita T, Kasahara K, et al. UVB Exposure Prevents Atherosclerosis by Regulating Immunoinflammatory Responses. *Arterioscler Thromb Vasc Biol.* 2017;37(1):66-74.
9. Sakaguchi S, Yamaguchi T, Nomura T, Ono M. Regulatory T cells and immune tolerance. *Cell.* 2008;133(5):775-787.
10. Rudensky AY. Regulatory T cells and Foxp3. *Immunol Rev.* 2011;241(1):260-268.
11. Bour-Jordan H, Bluestone JA. Regulating the regulators: costimulatory signals control the homeostasis and function of regulatory T cells. *Immunol Rev.* 2009;229(1):41-66.
12. Abbas AK, Benoist C, Bluestone JA, et al. Regulatory T cells: recommendations to simplify the nomenclature. *Nat Immunol.* 2013;14(4):307-308.
13. Weiss JM, Bilate AM, Gobert M, et al. Neuropilin 1 is expressed on thymus-derived natural regulatory T cells, but not mucosa-generated induced Foxp3+ T reg cells. *J Exp Med.* 2012;209(10):1723-1742, S1721.
14. Benson MJ, Pino-Lagos K, Roseblatt M, Noelle RJ. All-trans retinoic acid mediates enhanced T reg cell growth, differentiation, and gut homing in the face of high levels of co-stimulation. *J Exp Med.* 2007;204(8):1765-1774.
15. Haribhai D, Williams JB, Jia S, et al. A requisite role for induced regulatory T cells in tolerance

based on expanding antigen receptor diversity. *Immunity*. 2011;35(1):109-122.16. Josefowicz SZ, Niec RE, Kim HY, et al. Extrathymically generated regulatory T cells control mucosal TH2 inflammation. *Nature*. 2012;482(7385):395-399.17. Kim BS, Kim IK, Park YJ, et al. Conversion of Th2 memory cells into Foxp3+ regulatory T cells suppressing Th2-mediated allergic asthma. *Proc Natl Acad Sci U S A*. 2010;107(19):8742-8747.18. Amarnath S, Mangus CW, Wang JC, et al. The PDL1-PD1 axis converts human TH1 cells into regulatory T cells. *Sci Transl Med*. 2011;3(111):111ra120.19. Silpa-Archa N, Weerasubpong P, Junsuwan N, Yothachai P, Supapueng O, Wongpraparut C. Treatment outcome and persistence of repigmentation from narrow-band ultraviolet B phototherapy in vitiligo. *J Dermatolog Treat*. 2019;30(7):691-696.20. Ye J, Huang H, Luo G, et al. NB-UVB irradiation attenuates inflammatory response in psoriasis. *Dermatol Ther*. 2020;33(4):e13626.21. Tintle S, Shemer A, Suarez-Farinas M, et al. Reversal of atopic dermatitis with narrow-band UVB phototherapy and biomarkers for therapeutic response. *J Allergy Clin Immunol*. 2011;128(3):583-593 e581-584.22. Kemeny L, Varga E, Novak Z. Advances in phototherapy for psoriasis and atopic dermatitis. *Expert Rev Clin Immunol*. 2019;15(11):1205-1214.23. Bernard JJ, Gallo RL, Krutmann J. Photoimmunology: how ultraviolet radiation affects the immune system. *Nat Rev Immunol*. 2019;19(11):688-701.24. Vieyra-Garcia PA, Wolf P. A deep dive into UV-based phototherapy: Mechanisms of action and emerging molecular targets in inflammation and cancer. *Pharmacol Ther*. 2021;222:107784.25. Chen W, Jin W, Hardegen N, et al. Conversion of peripheral CD4+CD25- naive T cells to CD4+CD25+ regulatory T cells by TGF-beta induction of transcription factor Foxp3. *J Exp Med*. 2003;198(12):1875-1886.26. Xu L, Kitani A, Strober W. Molecular mechanisms regulating TGF-beta-induced Foxp3 expression. *Mucosal Immunol*. 2010;3(3):230-238.27. Akamatsu M, Mikami N, Ohkura N, et al. Conversion of antigen-specific effector/memory T cells into Foxp3-expressing T(reg) cells by inhibition of CDK8/19. *Sci Immunol*. 2019;4(40):28. Turner M, Mee PJ, Walters AE, et al. A requirement for the Rho-family GTP exchange factor Vav in positive and negative selection of thymocytes. *Immunity*. 1997;7(4):451-460.29. Tybulewicz VL, Ardouin L, Prisco A, Reynolds LF. Vav1: a key signal transducer downstream of the TCR. *Immunol Rev*. 2003;192:42-52.30. Korn T, Fischer KD, Girkontaite I, Kollner G, Toyka K, Jung S. Vav1-deficient mice are resistant to MOG-induced experimental autoimmune encephalomyelitis due to impaired antigen priming. *J Neuroimmunol*. 2003;139(1-2):17-26.31. Xu T, Stewart KM, Wang X, et al. Metabolic control of T(H)17 and induced T(reg) cell balance by an epigenetic mechanism. *Nature*. 2017;548(7666):228-233.32. Aso K, Kono M, Kanda M, et al. Itaconate ameliorates autoimmunity by modulating T cell imbalance via metabolic and epigenetic reprogramming. *Nat Commun*. 2023;14(1):984.33. Jordens I, Marsman M, Kuijl C, Neeffjes J. Rab proteins, connecting transport and vesicle fusion. *Traffic*. 2005;6(12):1070-1077.34. Grosshans BL, Ortiz D, Novick P. Rabs and their effectors: achieving specificity in membrane traffic. *Proc Natl Acad Sci U S A*. 2006;103(32):11821-11827.35. Yang CW, Hojer CD, Zhou M, et al. Regulation of T Cell Receptor Signaling by DENND1B in TH2 Cells and Allergic Disease. *Cell*. 2016;164(1-2):141-155.36. Oliveira VG, Caridade M, Paiva RS, Demengeot J, Graca L. Sub-optimal CD4+ T-cell activation triggers autonomous TGF-beta-dependent conversion to Foxp3+ regulatory T cells. *Eur J Immunol*. 2011;41(5):1249-1255.37. Lu CH, Wu CJ, Chan CC, et al. DNA Methyltransferase Inhibitor Promotes Human CD4(+)CD25(h)FOXP3(+) Regulatory T Lymphocyte Induction under Suboptimal TCR Stimulation. *Front Immunol*. 2016;7:488.38. Li MO, Rudensky AY. T cell receptor signalling in the control of regulatory T cell differentiation and function. *Nat Rev Immunol*. 2016;16(4):220-233.39. Serr I, Furst RW, Achenbach P, et al. Type 1 diabetes vaccine candidates promote human Foxp3(+)Treg induction in humanized mice. *Nat Commun*. 2016;7:10991.40. Nussbaum L, Chen YL, Ogg GS. Role of regulatory T cells in psoriasis pathogenesis and treatment. *Br J Dermatol*. 2021;184(1):14-24.41. Kim J, Moreno A, Krueger JG. The imbalance between Type 17 T-cells and regulatory immune cell subsets in psoriasis vulgaris. *Front Immunol*. 2022;13:1005115.42. Lee BH, Bang YJ, Lim SH, et al. High-dimensional profiling of regulatory T cells in psoriasis reveals an impaired skin-trafficking property. *EBioMedicine*. 2024;100:104985.

FIGURE LEGENDS

Figure 1 The therapeutic response of psoriasis patients treated with UVB is dictated by a specific cluster of CD4⁺ expressing Treg and TCR-activated markers. (A) UMAP of CD4⁺ T cells showing a distinct cluster of CD25⁺FOXP3⁺CD127⁺ cells (cluster 11) by CyTOF analysis. (B) Heatmap showing the differences among

clusters in CD4⁺ T cells. Each row represents the median arcsinh-transformed intensities in each cluster, and each column represents a marker. (C) Receiver operating characteristic (ROC) curve for the percentage of cluster 11 at baseline predicting UVB treatment response. Models were fit using logistic regression, both unadjusted (blue) and adjusted for gender and age (red). (D) Change in the percentage of cluster 11 CD4⁺T cells before (pre-UVB) and after (post-UVB) UVB treatment (n = 19). The P value was calculated using the Wilcoxon signed-rank test. PASI: Psoriasis Area Severity Index. (E) Left: Biaxial contour plots illustrating the distribution of HLADR-TIGIT and HLADR-TIM3 expressing cells within cluster 11, pre- and post-UVB treatment. Numbers indicate the percentage of cells in each quadrant. Right: Paired Wilcoxon signed-rank tests were used to compare the frequencies of HLADR^{hi}TIGIT^{hi} and HLADR^{hi}TIM3^{hi} cells in cluster 11 before and after UVB treatment.

Figure 2 UVB alleviates OVA-induced inflammatory responses in the skin by increasing OVA-specific Treg cells. (A) Mice were intraperitoneally injected with OVA/alum on days 0, 7, and 14 and epicutaneously treated with OVA patches on day 14. The mice were exposed to UVB every other day three times during the OVA patch application. (B) Images of mouse dorsal skin are shown. (C) Changes in transepidermal water loss (TEWL). n = 5 for the ctrl and O groups; n = 3 for O+U groups. (D) Histological changes within the graft were assessed using hematoxylin and eosin staining. (E-G) Flow cytometry of cells isolated from skin and draining lymph nodes (LNs). Cells isolated from the skin were restimulated. IL-4, IL-5, and IL-22 in CD4⁺ T cells were analyzed (E). CD25⁺Foxp3⁺ Treg cells and the markers associated with TCR activation were analyzed in cells isolated from skin-draining LNs (F). Cells from the skin were incubated with the OVA₃₂₃₋₃₃₉ tetramers, followed by the antibodies against the indicated markers. OVA-specific Treg cells were analyzed (G). Statistical analyses: one-way ANOVA with Kruskal-Wallis test. Mean ± SEM. *, p<0.05; **, p<0.01; ***, p<0.001.

Figure 3 UVB prolongs allograft survival by inducing allograft-specific Treg cells. (A) Schematic depicting the allograft transplantation experiment. Mice were treated with UVB on alternating days starting on day 5 (d5) for five treatments post-transplantation. n = 9 for the No UVB group; n = 8 for the UVB group. (B) Skin grafts were monitored from d5 post-transplantation. Grafts were considered rejected when less than 20% viable tissue remained. (C) Histological changes within the graft were assessed using hematoxylin and eosin staining. (D) Flow cytometry of cells isolated from the grafts. CD25⁺Foxp3⁺ Treg cells and ICOS, CTLA-4, and LAG-3 expression were analyzed. (E) Schematic diagram of the second allograft transplantation. Recipient mice, previously subjected to a first allograft transplant with or without UVB treatment, received a second allograft from either C57BL/6 or C3H mice. (F) Skin graft appearance was monitored until rejection. n = 5 for each of the groups. Statistical analyses: Gehan-Breskiw-Wilcoxon test. *, p<0.05; **, p<0.01; ****, p<0.0001.

Figure 4 Antigen-specific Treg cells affect clinical outcomes of inflammatory skin diseases. (A) Scatter plot illustrating the correlation between the percentage of cluster 11 in CD4⁺ T cells and PASI score in psoriasis patients. The P value was calculated using Spearman's correlation. (B) Box-and-whisker plot comparing the percentage of cluster 11 in CD4⁺ T cells in healthy controls (HC) and psoriasis patients with low (PASI [?] 4.5), medium (4.5 < PASI < 9), and high (PASI [?] 9) disease severity. PASI: Psoriasis Area Severity Index. (C) Foxp3^{DTR-GFP} Mice were sensitized with OVA/alum, challenged by the OVA patch, and treated with UVB. CD25⁺GFP⁺ Treg cells were sorted from the skin-draining LNs. CD4⁺GFP⁺T cells as responder T cells were sorted from the skin-draining LNs of OTII/Foxp3^{DTR-GFP} mice. Treg and responder T cells were mixed at a ratio of 1 to 1 and then were administered to the recipient mice by intravenous injection. The recipient mice were then sensitized with OVA/alum by intraperitoneal injection and challenged with the OVA patches. (D) TEWL was measured every other day. n = 3 for each of the groups. (E) Histological changes within the graft were assessed using hematoxylin and eosin staining. (F) Cells isolated from the skin were restimulated. IL-5 production on CD4⁺ T cells was analyzed. (G) Sorted CD25⁺GFP⁺ Treg cells from mice with OVA stimulation and UVB treatment were intravenously injected into the recipient mice. The ears of the mice were then stimulated with 15 mg of imiquimod-containing cream. (H) Changes in the ear swelling of mice were shown. n = 4 for each of the groups. (I) Cells isolated from ears were restimulated. IL-17 and IL-22 on CD4⁺ T cells were analyzed. Statistical analyses: one-way ANOVA with Kruskal-Wallis

test. P for trend test was calculated by ordinary one-way ANOVA. Mean \pm SEM. *, $p < 0.05$; **, $p < 0.01$; ***, $p < 0.001$.

Figure 5 UVB enhances genes involved in cell stability, cell proliferation, and cellular localization, and suppresses genes associated with negative regulation of Treg development. (A) Pathway analysis of upregulated genes in Tregs from skin of mice treated with UVB compared to those of mice without UVB treatment ($n = 2$ treated and $n = 2$ untreated, pooled samples). GOBP: Gene Ontology Biological Process; NES: Normalized Enrichment Score. (B) UMAP plot of $CD4^+$ T cells from patients PBMC samples (2 patients, with pre- and post-treatment samples). (C) Dot plot of gene markers for Treg, T memory, T effector, and naive T clusters. (D) Heatmap showing gene expression changes in $CD4^+$ Tregs from mice and human PBMC under UVB treatment. (E) Violin plot of negatively-associated genes (*RAB35*, *IDH1*, and *VAV1*) with significant gene expression changes ($p < 0.05$) in human PBMC-derived Treg cells under UVB treatment. Statistical significance was tested through the Wilcoxon ranked test.

Figure 6 Treg transition from human $CD4^+$ T cell lineage and clonal expansion under UVB treatment. (A-D) Analyses of $CD4^+$ T cells obtained from the periphery of psoriasis patients treated with UVB and the public dataset generated from healthy human skin. UMAP of $CD4^+$ T cell clusters with an overlaid Slingshot trajectory (A). UMAP plot of 9375 $CD4^+$ T cells in the skin with Slingshot trajectory (B). A chronologically color-coded pseudotime UMAP of $CD4^+$ T cells from violet (least differentiated) to yellow (most differentiated) (C). Expression of key genes for pseudotime trajectory, color coded by the clusters shown in panel A (D). (E) (Left) UMAP visualization of $CD4^+$ T cell subtypes. (Right) Clonal expansion overlay on the UMAP, with higher density indicating greater clonal expansion. (F) Distribution of clonal size across four $CD4^+$ T cell subtypes under UVB treatment. Numbers represent cell counts in each condition. (G) Expansion indices were quantified using the STARTRAC-expa method.

Figure 1

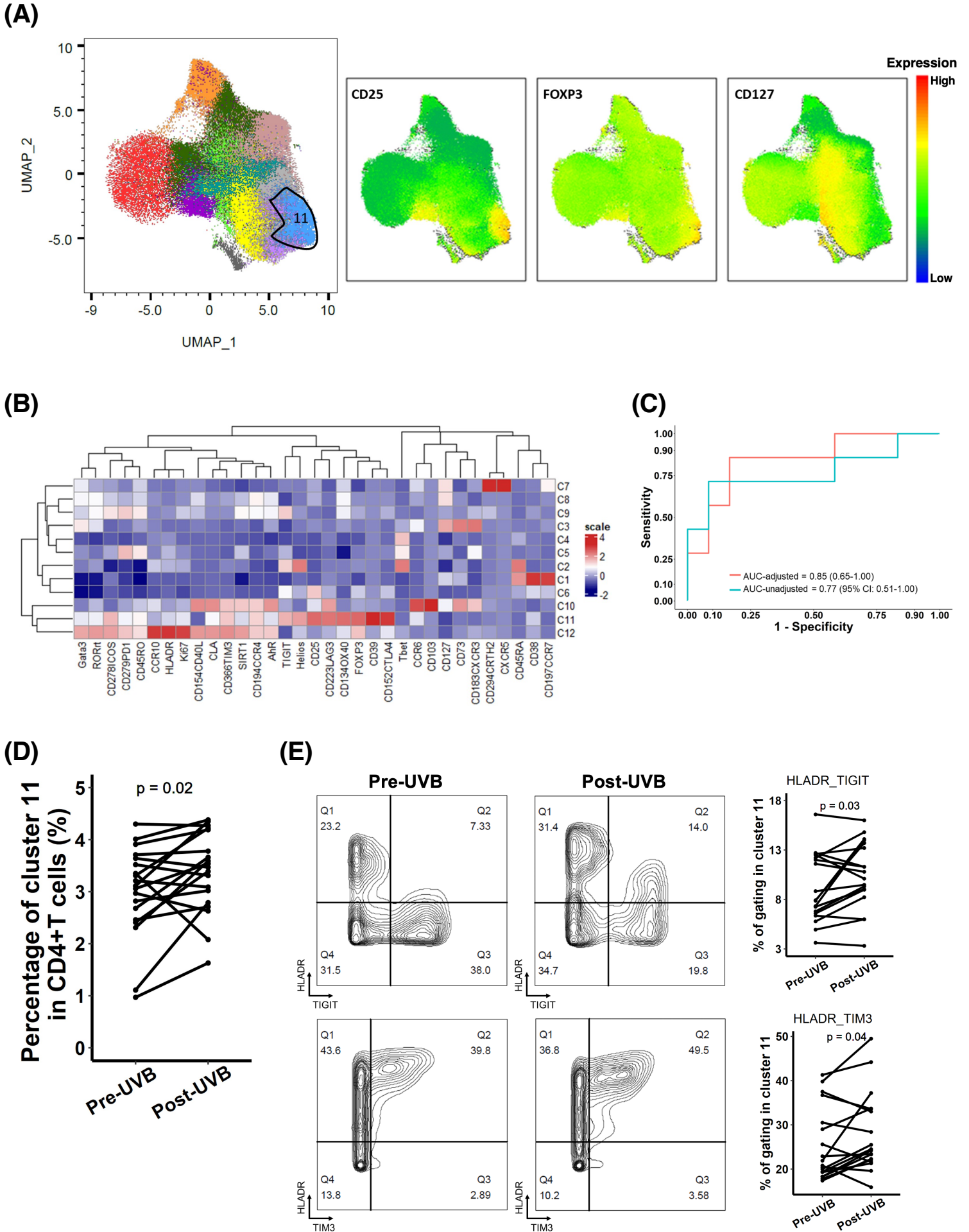


Figure 2

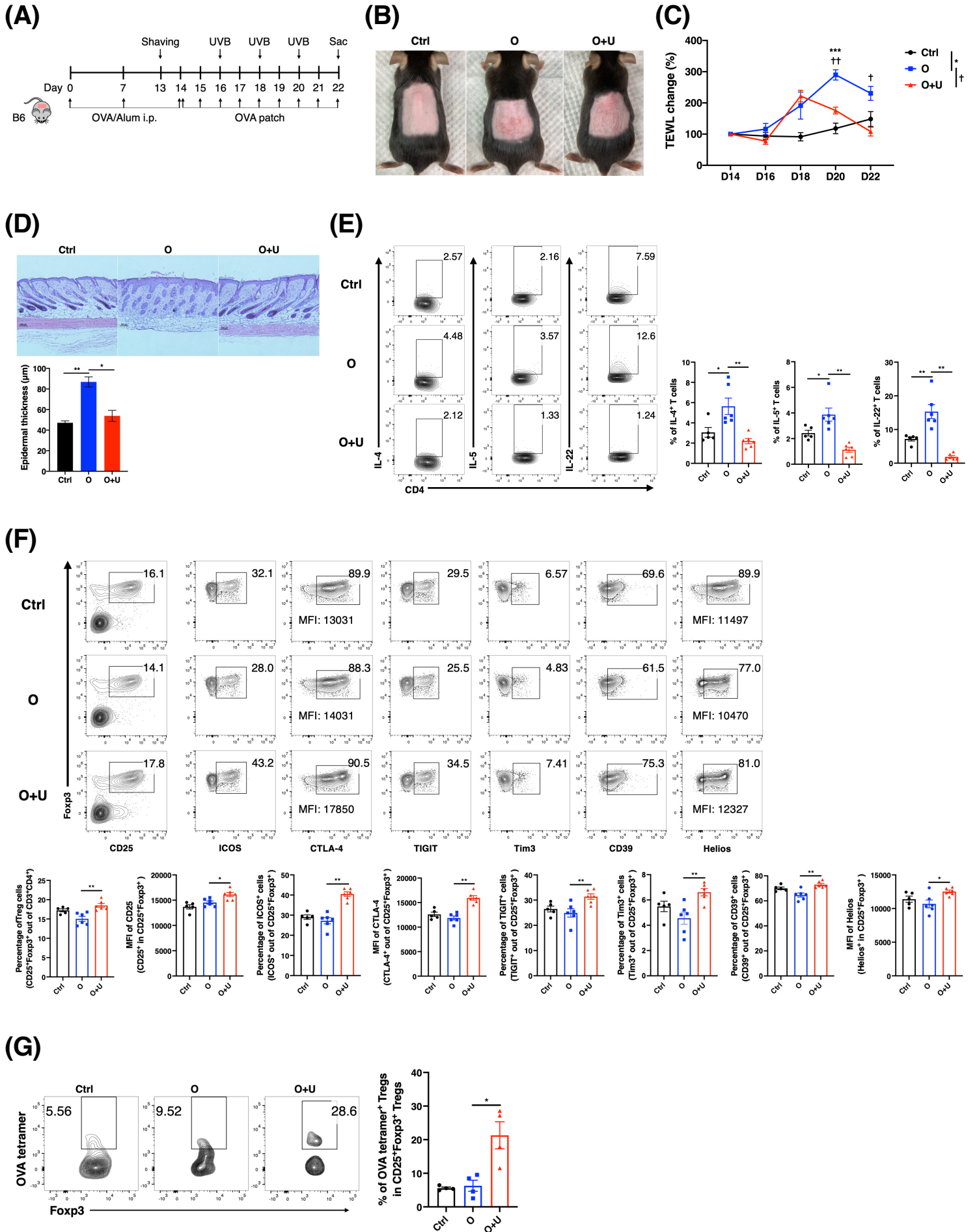


Figure 3

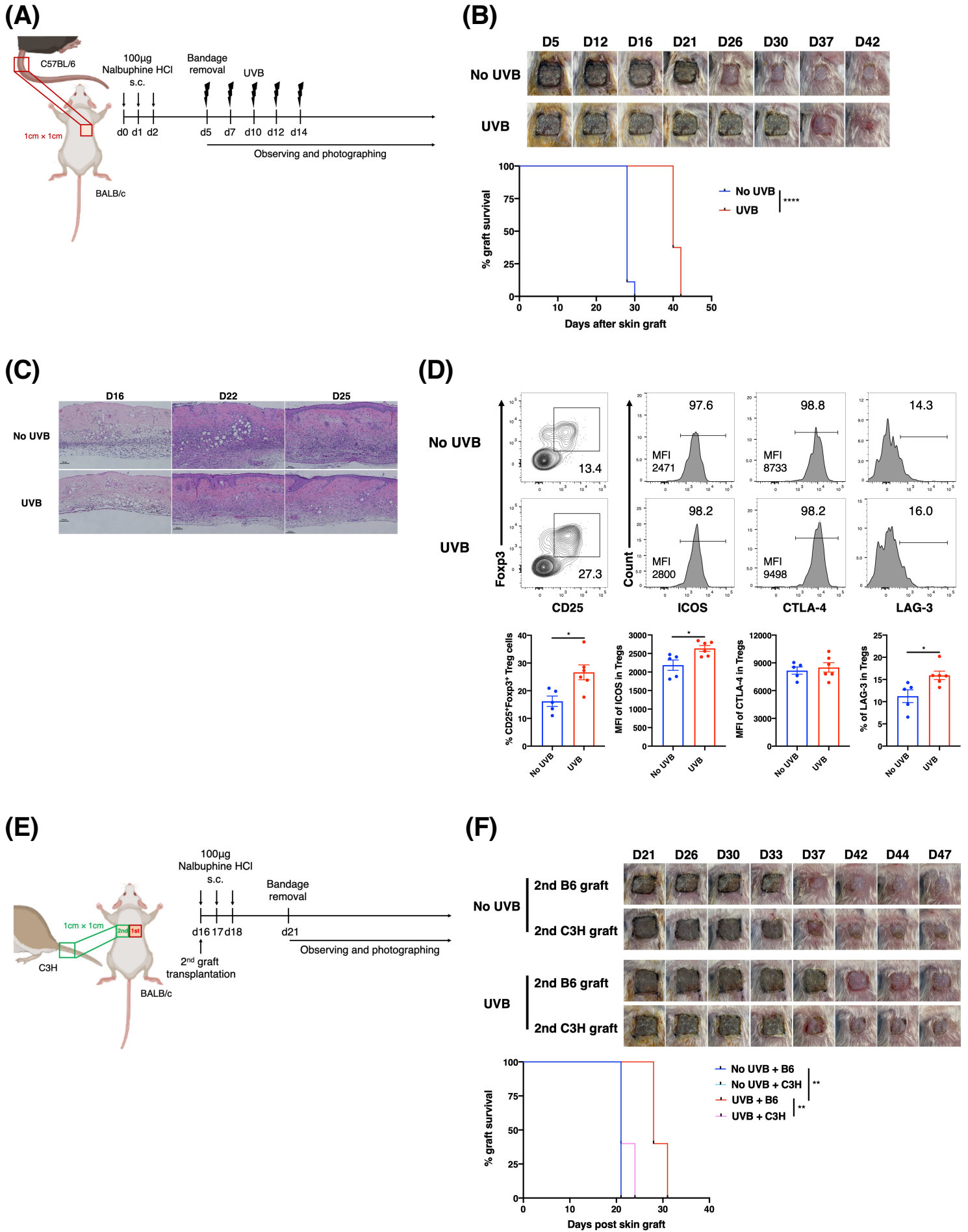


Figure 4

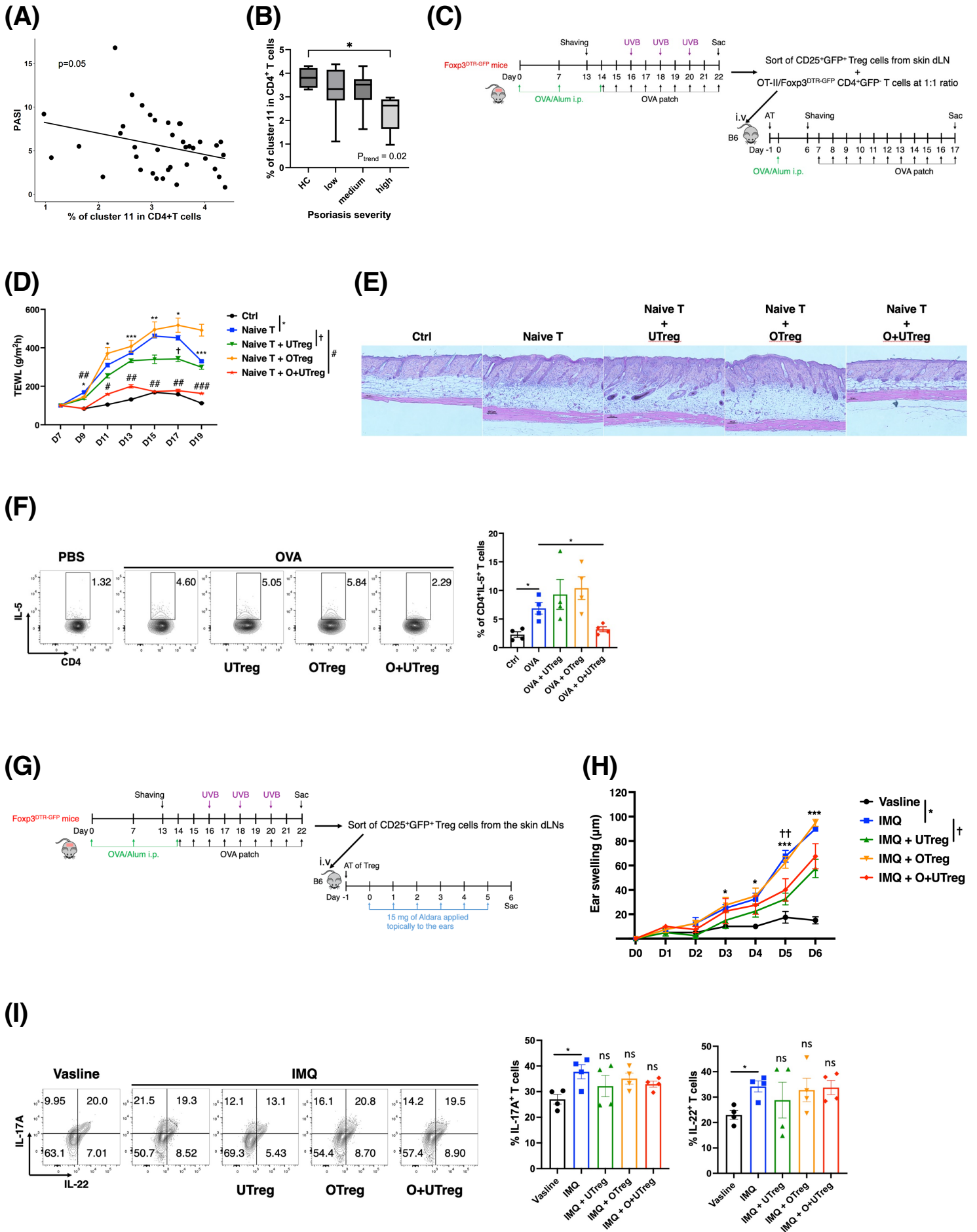
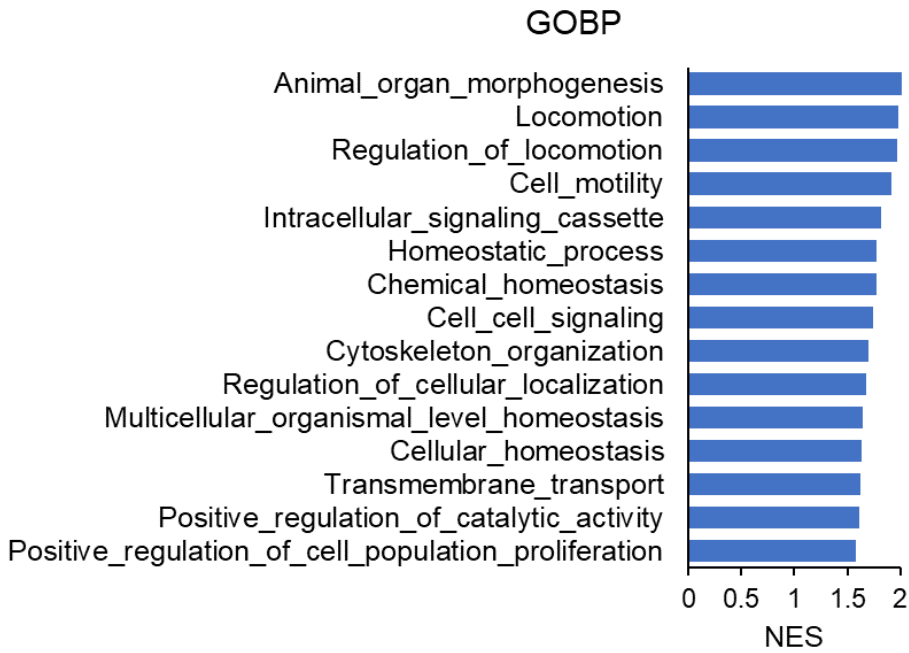
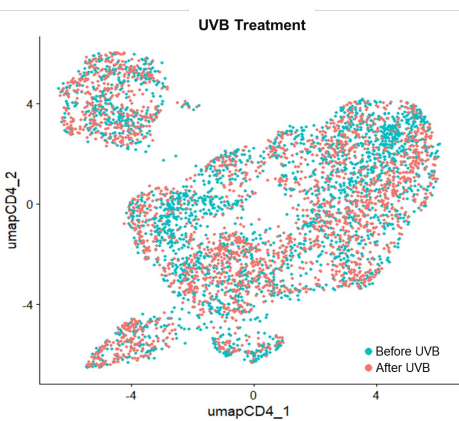


Figure 5

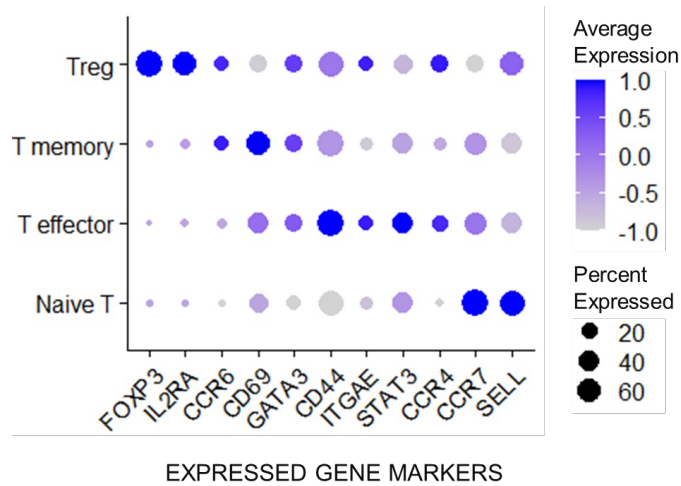
(A)



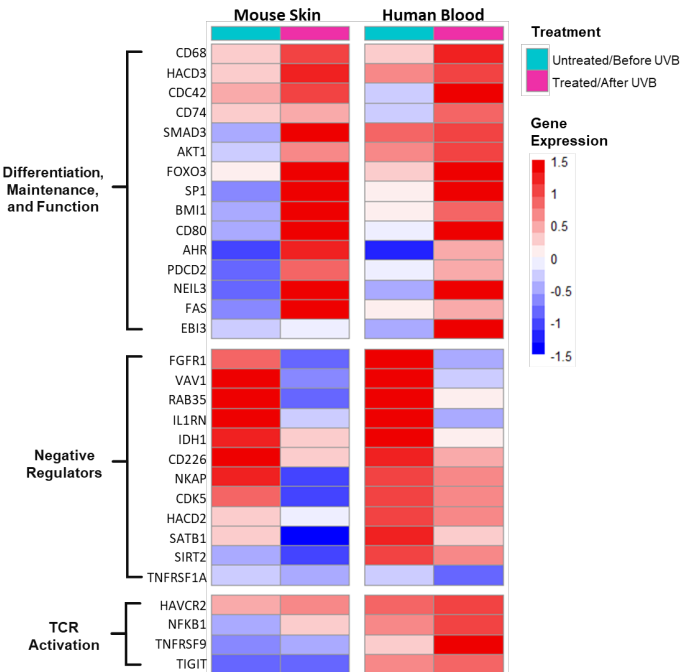
(B)



(C)



(D)



(E)

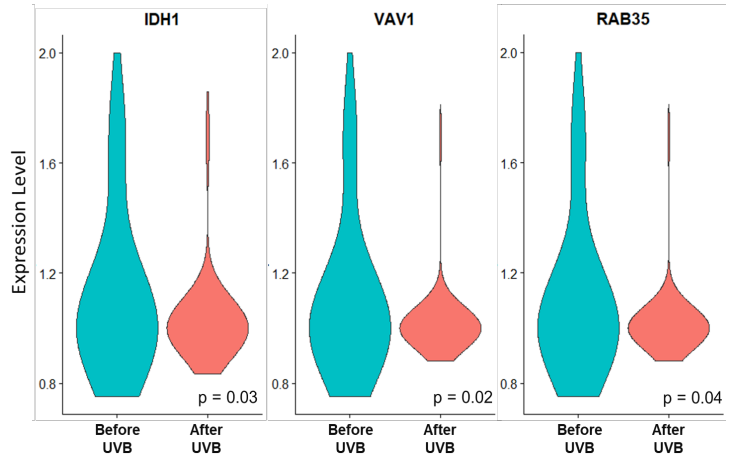
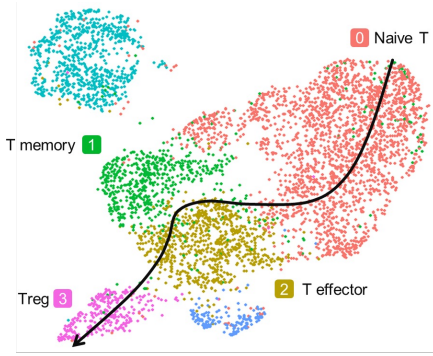
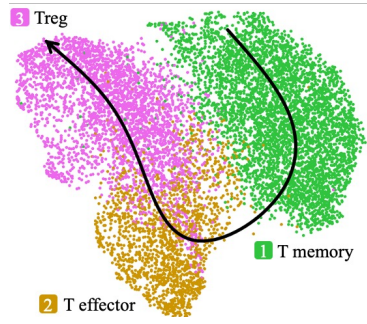


Figure 6

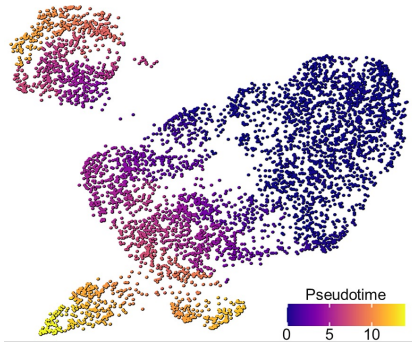
(A)



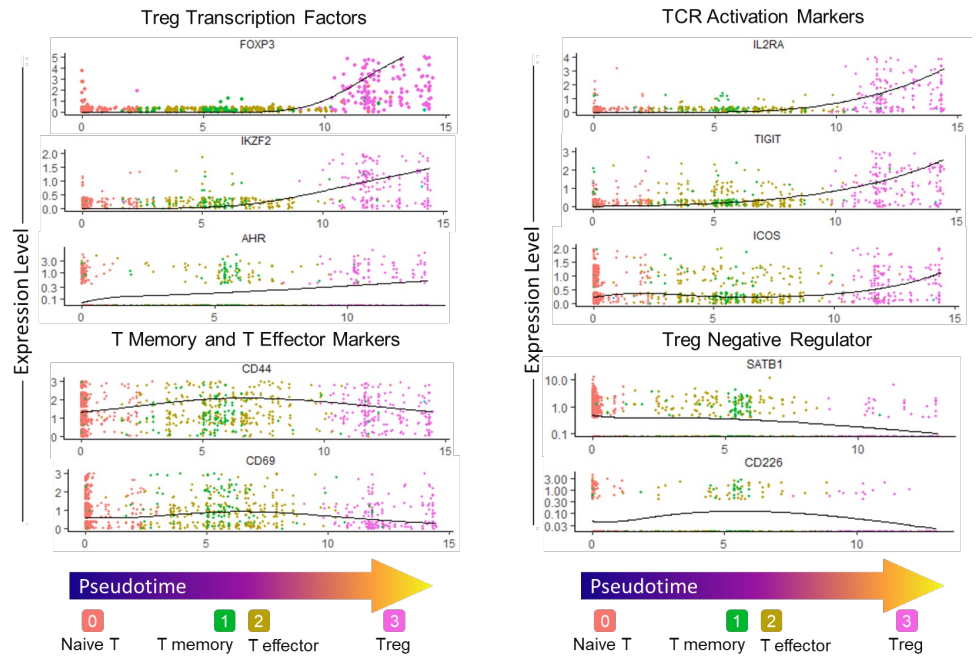
(B)



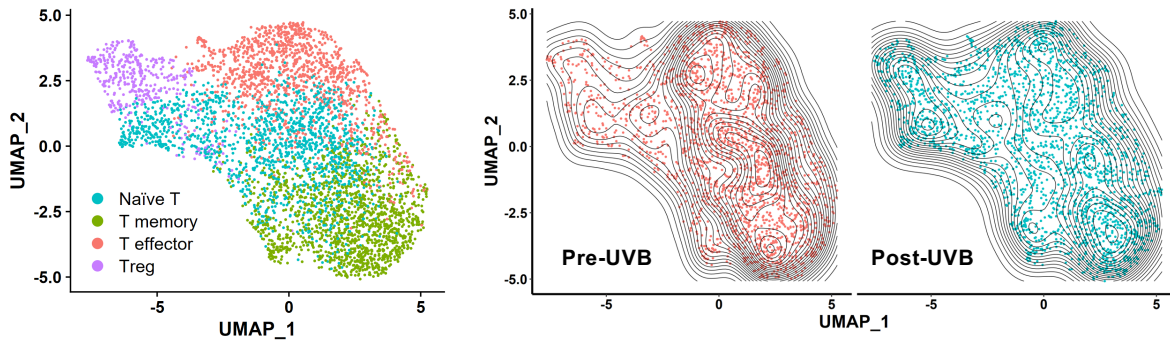
(C)



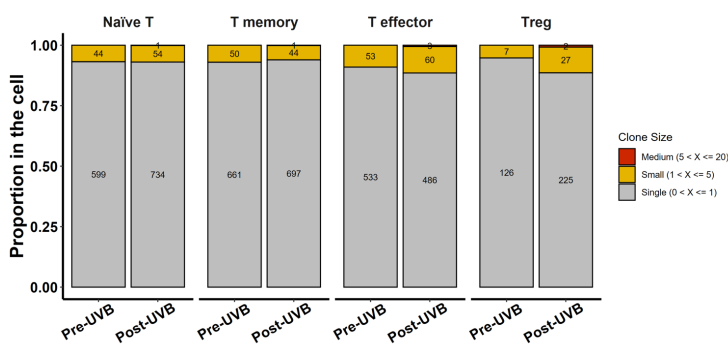
(D)



(E)



(F)



(G)

